Earthquake Engineering, Tenth World Conference © 1992 Balkema, Rotterdam. ISBN 90 5410 060 5

Pseudo-dynamic tests on composite steel/concrete joints

D.R.Constantinescu
Krebs & Kiefer Consulting Engineers, Darmstadt, Germany
J.van Kann, A.M.Pradhan, H.W.Ashadi & J.G.Bouwkamp
Institute of Steel Construction, Technical University Darmstadt, Germany

ABSTRACT : The paper presents the results of numerical and experimental studies carried out to design the test specimens and to choose the dynamic excitation for a research programme aiming at investigating both the seismic behaviour of composite beam-column joints and the reliability of pseudodynamics test technique. The preliminary pseudo-dynamics tests confirmed in general the numerical assessment but emphasized, however, the need to improve the hysteretic model for the panel zone.

1 INTRODUCTION

The work reported within the paper is part of a research programme on the earthquake response of beam-column connections of composite steel-concrete moment-resisting frames. The programme has been proposed within the W.G.3 'Composite Steel- Concrete Structures' of the European Association of Structural Mechanics Laboratories at the EC - Joint Research Centre ISPRA and is being carried out by a multi-national team of research institutions from Belgium, Germany and Greece. Two major aims are envisaged: (i) to investigate the reliability of the pseudo-dynamic tests in capturing the earthquake response of composite structures in particular when different relative contributions of the steel and concrete parts to the stiffness and load-bearing capacity are involved and (ii) to get experimental evidence on the dynamic behaviour of beam-column composite connections of earthquake resisting frames and investigate the ability of existing numerical models to capture this behaviour.The former research aim will be achieved by comparing the results of pseudo-dynamic tests with results of tests carried out on a shaking table.

The test specimen is depicted in Fig.1. It models an external joint of a multistory frame with a bay span of about 8 m and a story heigth of about $3m$. The steel sections of the beam and column are HE 260 A and HE 300 B, respectively. The column including the shear panel and the end part of the beam are filled in with concrete reinforced with a welded mat ($\phi 6.5mm/15cm$). A mass of 4 *tons* is taken at the column top. As the specimen mass is relatively small, it is assumed that the system has one degree-of-freedom.

Both welded as well as bolted beam-column connections are to be tested. In order to vary the relative contribution of steel and concrete within the shear panel, the steel web is to have three different thicknesses: (1) normal, i.e. 11 mm, (2) reduced to 7 mm by machining out and (3) increased to 15 mm by welding of an additional steel plate. Hence, six different test specimens are to be investigated. In total 45 specimens are to be tested within the research programme.

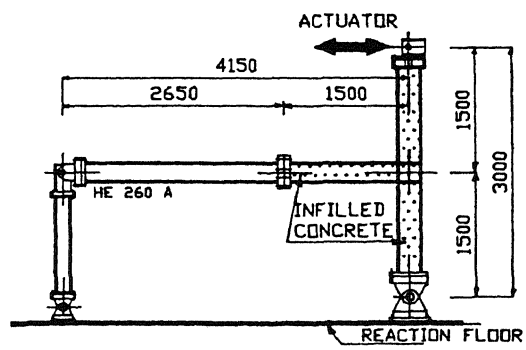

Fig.1 Test specimen and setup.

Three pseudo-dynamic tests have been already carried out. The paper presents the results of these tests as well as of the numerical studies performed prior and after the tests.

2 TEST DESIGN

To assess whether the specimen yielding is to be governed by the shear panel or by the beam, the shear force in the shear panel, Q, associated to each of the two above mentioned plastic mechanisms are first

computed and compared.

(i) The shear force $[kN]$ associated with the beam yielding is given by (Fig.2a)

$$Q_{by} = \frac{M_y}{0.2375} - Q_c = 3.24\sigma_y \qquad (1)$$

where M_y $[kNm]$ denotes the yield moment of the beam, Q_c the column shear force and σ_y [N/mm2] the yield strength of steel. A $\sigma_y = 300N/mm^2$ is characteristic for the used steel grade (St37), so that $Q_{by} = 930$ kN.

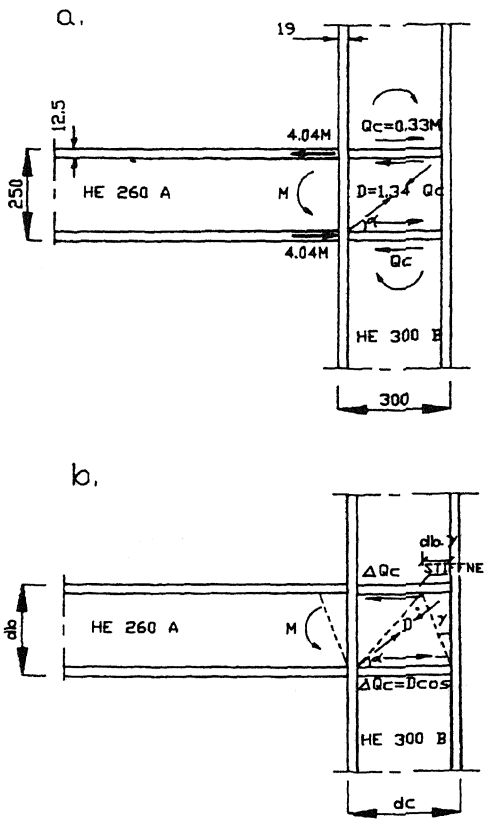

Fig.2 Shear strength and deformation of panel zone.

(ii) Both steel and concrete contribute to the shear panel strength (Fig.3).

The steel contribution will be first assessed. The state A' of the bilinear relationship between the steel shear force and the shear panel distorsion, γ, corresponds to the shear yielding of the web. As

$$Q_{sy} = \frac{d_c t_w \sigma_{wy}}{\sqrt{3}} \qquad (2)$$

and

$$\gamma_y = \frac{\sigma_{wy}}{\sqrt{3}G} \qquad (3)$$

where d_c is the depth of the column section, t_w is the steel web thickness and σ_{wy} is the yield strength of steel in the web. Based on experimental evidence it can be assumed that $\sigma_{wy} \approx 1.1\sigma_y = 330N/mm^2$, so that

$$Q_{sy}[kN] = 571.6t_w[cm] \qquad (4)$$

and $\gamma_y = 2.28mm/m$. The strength increase ΔQ_s beyond the state A' is mainly caused by the bending of the column flanges bounding the panel zone (Krawinkler 1987) and can be computed with

$$Q_s = \frac{1.9b_f t_f^2 \sigma_y}{d_b} \qquad (5)$$

in which b_f and t_f denote the width and thickness of the column flange and d_b is the beam depth. Eq.(5) yields $\Delta Q_s = 237.4kN$.

The contribution of the concrete diagonal strut to the shear strength of the panel zone is denoted by ΔQ_c . The geometric relationship between the diagonal compressive strain ϵ and the panel distortion (Fig.2b)

$$\epsilon = 0.5\gamma \sin 2\alpha = 0.497\gamma \qquad (6)$$

yields $\epsilon = 1.13mm/m$ when $\gamma = \gamma_y$, which means that the concrete strut will reach about 81% of its

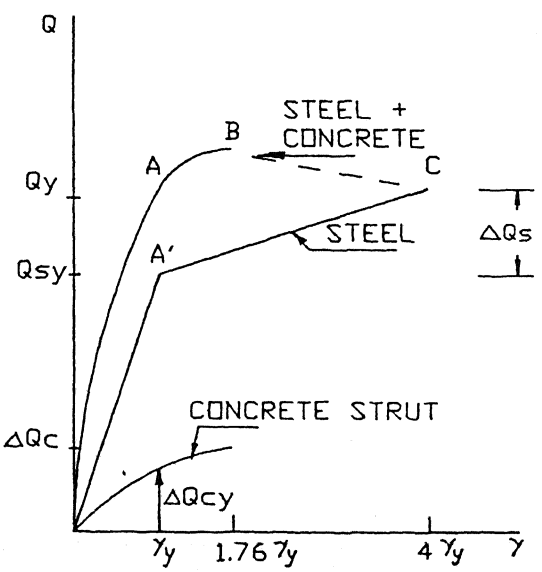

Fig.3 Contribution of steel and concrete to the relationship between the shear force, Q, and shear distorsion, γ, of the composite panel zone.

compressive strength, $D_u = 2A_c f_{ck}$, when the state A in Fig.3 is reached. A_c denotes the strut cross section on oneside of the web and f_{ck} is the compressive concrete strength. Assuming that $A_c = 200cm^2$, which correspond to a strut width of about half of the diagonal length, and accounting that the chosen concrete has $f_{ck} \approx 17.5N/mm^2$ it follows that $Q_{cy} \approx 380kN$.

The superposition of both steel and concrete contributions to the shear behaviour of the panel zone follows as depicted in Fig.3. It is apparent that the yielding of steel web always preceedes the attainment of the concrete strut strength. The previous results are depicted in Fig.4.

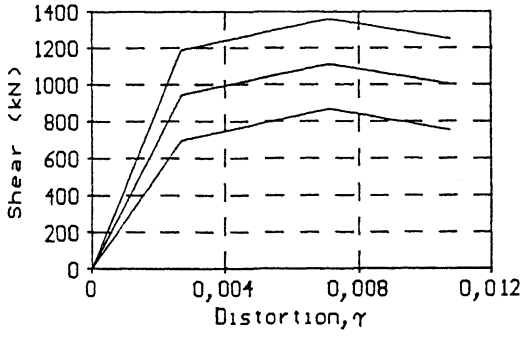

Fig.4 Q - γ relationships for panel zones with t_w = 7, 11 and 15 mm.

The comparison of Q_y with Q_{by} shows that the plastic deformation of the test specimen would occur (i) mainly within the panel zone, when $t_w = 7mm$, (ii) both within the panel zone and the beam end zone, when $t_w = 11mm$ and (iii) mainly within the beam end zone, when $t_w = 15mm$. A variety of nonlinear test conditions could therefore be achieved by choosing the three different web thicknesses within the panel zone. It is however apparent that the numerically evaluated Q_y and Q_{by} are very close to each other and that this assessment should have been checked experimentally before starting the execution of all test specimens.

Two types of ground motions are to be used in the dynamic tests: a cyclic excitation with a linearly increased amplitude and an earthquake excitation. The time-history of the former ground displacement can be analytically described by means of the relation

$$u = u_0(t)\sin(2\pi t/T) \qquad (7)$$

where T denotes the period (constant) and u_0 the amplitude envelope. Ground motions as depicted in Fig.5 were envisaged, so that the ascending path, for instance, is given by (δ = constant)

$$u_0(t) = \delta \cdot t \qquad (8)$$

The magnitude of the nonlinear dynamic response of the test specimen can therefore be influenced by means of T and u_0. These parameters were so chosen as to maximize the plastification of the test specimen without violating the performances of the shaking table. It is worth noting that the relationships between the maximum values of the displacement, max.u, velocity, max.v, and acceleration, max.a, of the chosen ground motion are given by $max.v = max.u \cdot (2\pi/T)$ and $max.a = max.v \cdot (2\pi/T)$. The choice of the period T is therefore crucial. The effect of the ratio $\frac{T}{T_0}$, where T_0 is the fundamental period of the test specimen, when the ground motion were harmonic, is depicted in Fig.6. Parametric studies were carried out with the numerical model described in the next section to optimize the characteristics T and δ.

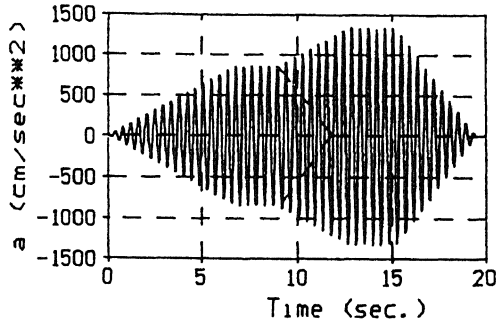

Fig.5 Chosen ground motion.

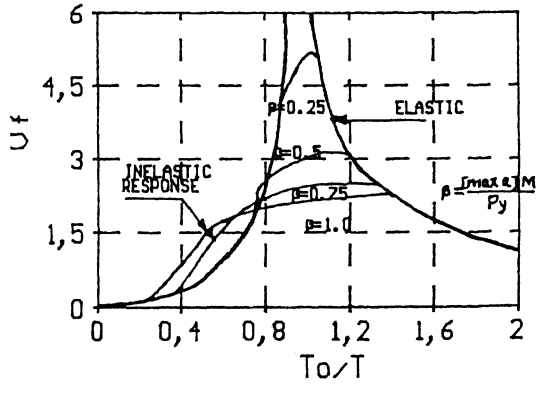

Fig.6 The dynamic amplification of the displacement amplitude (V_f = relative response / max.u) of SDOF systems with mass M and yield force P_y under harmonic ground motion (Bouwkamp 1989).

They led to the ground motion depicted in Fig.5 with $T = 0.433s$ ($T/T_0 \approx 0.8$). The maximum ground motion values to be reached during the dynamic excitation are $max.u = 6.3\ cm$, $max.v = 92cm/s$ and $max.a = 1.36g$.

3 NUMERICAL MODELLING

The test specimen was numerically modelled as depicted in Fig.7 and computed with the program ANSR (Mondkar 1975). The beam-column connection is modelled by means of undeformable beam-column and truss elements. The ANSR shear-link element (Ricles 1988) is used to model the panel zone. The moment - rotation relationship for this element was deduced from the Q - γ relationships in Fig.4. On account that the shear link inflexion point is always at midheight, the following conversions were used ($h = 23.75cm$)

$$2M = Q \cdot h \tag{9}$$

$$12EI = h^2 \frac{Q_y}{\gamma_y} \tag{10}$$

4 PSEUDO-DYNAMIC TESTS

Three preliminary pseudo-dynamic tests (Fig.8) have been carried out with welded specimens in order to check whether the selected design of specimens and the intended ground excitation will yield indeed the desired dynamic response of the specimens. The specimens with the web thicknesses $t_w = 11$ and 15 mm were tested using the entire length of the ground motion from Fig.5 (i.e. $max.u = 6.3cm$), while the specimen with $t_w = 7mm$ was tested using the broken-line envelope in Fig.5 (i.e. $max.u = 4.2cm$). The explicit Newmark algorithm ($\beta = 0, \gamma = 0.5$) with a numerical time increment $\delta t = 0.02s$ were used. The tests were conducted with an actuator velocity which was varied between 8 and 24 mm/s in order to check the sensivity of the analog controller too. A viscous damping of 1% was assumed. The frictional damping was measured prior to the test and was eliminated numerically on- line.

The experimental results are depicted in Fig.9. The global hysteretic behaviour of the test specimens is depicted by means of the relationship between the actuator force and displacement (Fig.9a), while the responses of the panel zone and of the beam are depicted in Fig.9b and c by means of the relationships $Q - \gamma$ and, respectively, $M - \Theta$.

The experimental results confirm the above mentioned assessment regarding the effects of the web

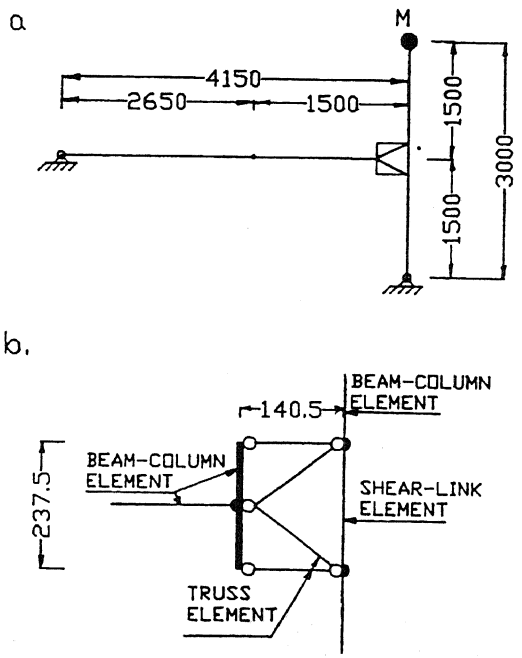

Fig.7 Numerical model (a) with detail of the beam-column joint (b).

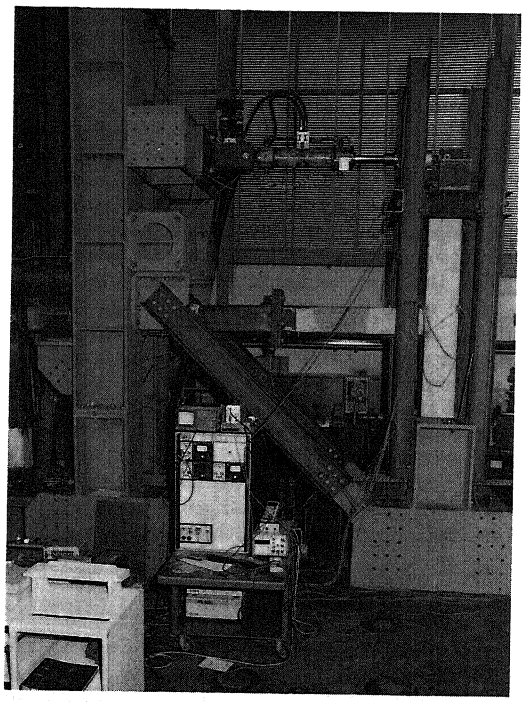

Fig.8 General view of the test.

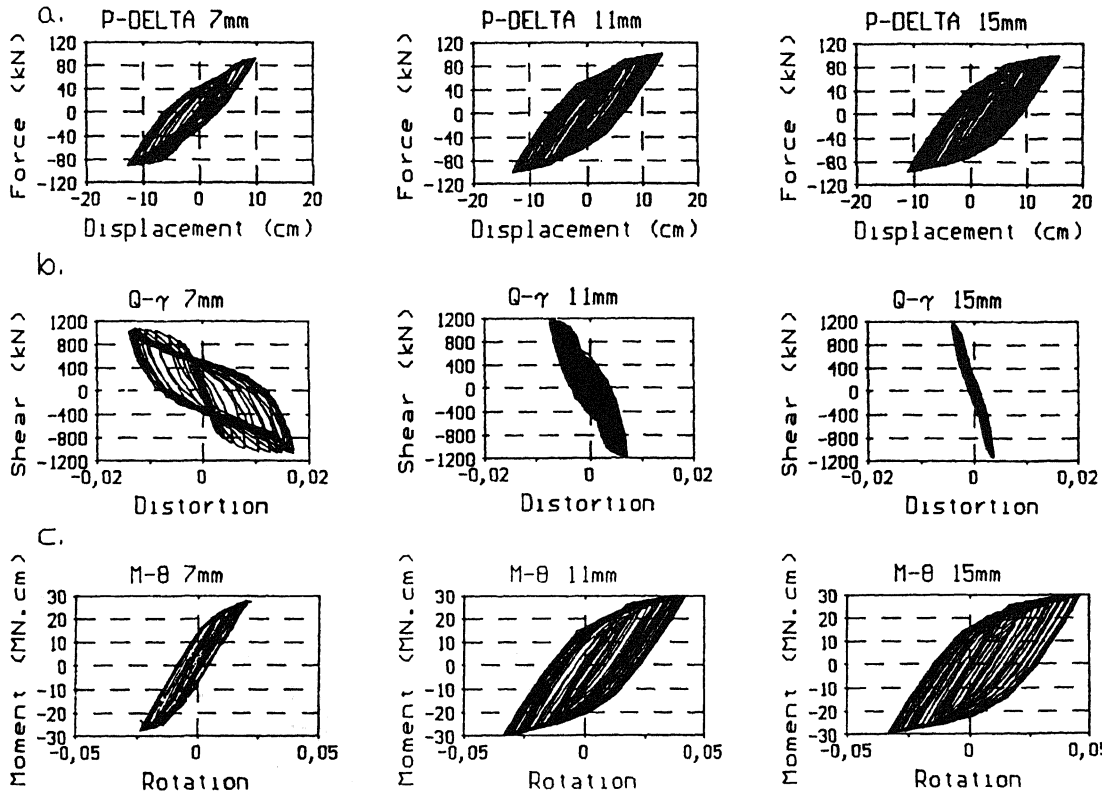

Fig.9 Pseudo-dynamic test results.

thickness t_w on the plastification of panel zone and beam. It is however worth mentioning that the three different t_w affect only the relative degree of plastification of the panel zone and of the beam, while the dynamic response of the system (Fig.9a) is practically the same. The tests also show the effectiveness of the chosen ground motion on the non-linear dynamic response of the test specimens. Thus, the input amplification factor (max. response (displacement) / max.u) is about 2.5 and the induced system plastification (max.response / yield displacement) is about 2.

5 COMPARISONS WITH NUMERICAL RESULTS

Results of the dynamic numerical modelling are confronted in Fig.10 with experimental results. The use of the Q - γ relationship from Fig.4 yields the results in Fig.10b. The relationships in Fig.10c correspond to a model in which the yield strength of the panel zone was artificially increased to avoid its plastification.

The following conclusions arise from comparing the results in Fig.10a and b.

1. Although the numerically assessed response of the system is in good agreement with the experimental evidence, the hysteretic behaviour of the two components, i.e. panel zone and beam, cannot be captured satisfactorily. Indeed, the experimental investigation shows that the panel zone is relatively less plastified as the beam, while the numerical model yields opposite results. That seems to be mainly due to the inadequacy with which the hysteretic behaviour of the shear panel is being modelled.

2. A hysteretic model with degrading stiffness rather than a non-degrading stiffness model must be implemented in order to capture the panel zone response. Models as depicted in Fig.11, e.g. with the reloading paths 4-5-6-7 or 4-7 (Takeda), will be adequate. The stiffness degradation which occurs by the reloading in opposite direction has to do with the in-filled concrete behaviour and may be due to the temporary loss of contact between steel stiffners and diagonal concrete strut (corner gap).

The importance of the adequate modelling of the shear panel behaviour is emphasized once again when the numerical results in Fig.10c are compared with those from Figs.10a and b. Indeed, it is apparent that the beam behaviour could be well captured if the panel zone response could be realistically modelled.

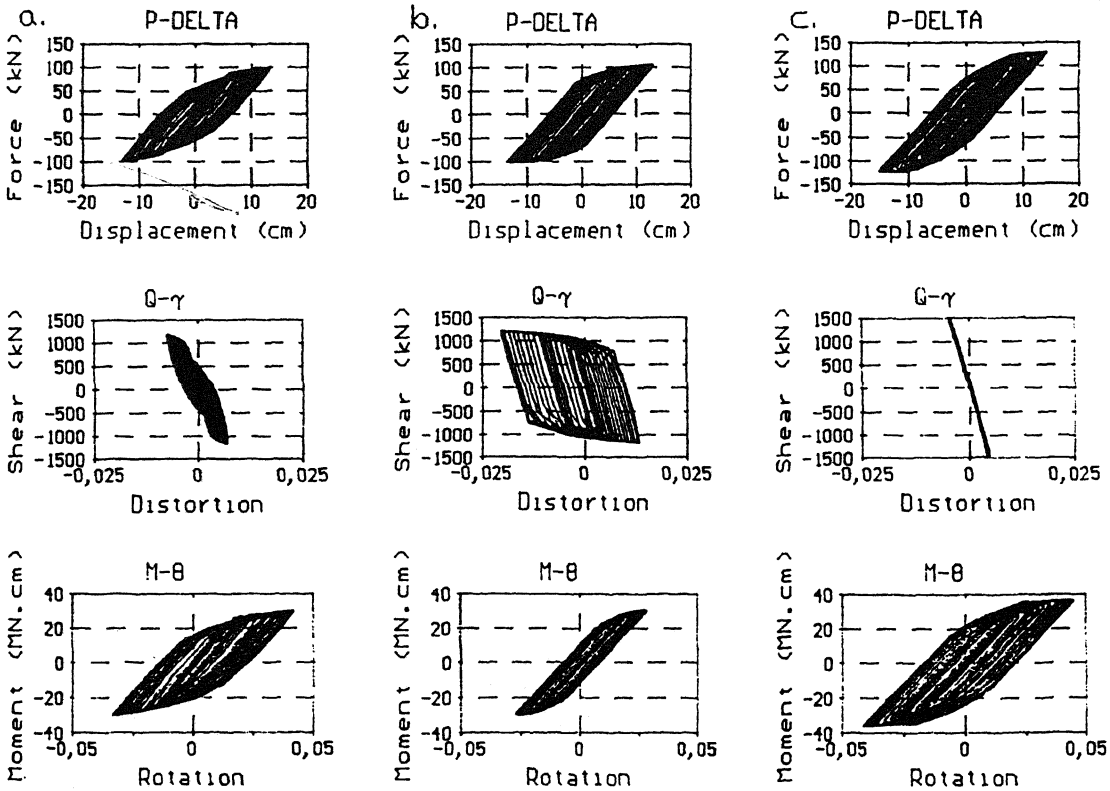

Fig.10 Comparison of experimental (a) and numerical results (b,c) for the test specimen with t_w = 11 mm.

6 CONCLUSIONS

The experimental evidence gathered by means of the pseudo-dynamic tests reported here have in general confirmed the findings of the numerical assessment carried out to design the test specimens and choose the optimum dynamic excitation. They also emphasized the need to better the numerical modelling of the panel zone of the composite beam-column connections.

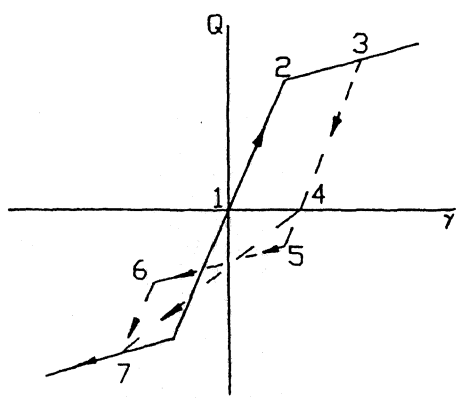

Fig.11 Hysteretic models for the composite panel zone

REFERENCES

Bouwkamp, J.G., D.R. Constantinescu & J. van Kann 1989. Ermittlung äquivalenter Dämpfungsmasse aus Antwortanalysen erdbebenerregter Rohrleitungssysteme. BMU Research Programme SR376. *Interim report.*

Krawinkler, H. & S. Mohasseb 1987. Effects of panel zone deformations on seismic response. *J. of Constr. Steel Research.* 8: 233-255.

Mondkar, D.P. & G.H. Powell 1975. ANSR-I a general purpose program for analysis of nonlinear structural response. *EERC-Report No.75-37.* Berkeley.

Ricles, J.M..1988. User's guide to an enhanced version of ANSR-1 *(manuscript)*